Chapter 9

Enhancement of Photosynthetic Productivity by Quantum Dots Application

Angela Janet Murray, John Love, Mark D. Redwood,
Rafael L. Orozco, Richard K. Tennant,
Frankie Woodhall, Alex Goodridge and
Lynne Elaine Macaskie

Additional information is available at the end of the chapter

http://dx.doi.org/10.5772/intechopen.74032

Abstract

The challenge of climate change promotes use of carbon neutral fuels. Biofuels are made via fixing carbon dioxide via photosynthesis which is inefficient. Light trapping pigments use restricted light wavelengths. A study using the microalga *Botryococcus braunii* (which produces bio-oil), the bacterium *Rhodobacter sphaeroides* (which produces hydrogen), and the cyanobacterium *Arthrospira platensis* (for bulk biomass) showed that photosynthetic productivity was increased by up to 2.5-fold by upconverting unused wavelengths of sunlight via using quantum dots. For large scale commercial energy processes, a 100-fold cost reduction was calculated as the break-even point for adoption of classical QD technology into large scale photobioreactors (PBRs). As a potential alternative, zinc sulfide nanoparticles (NPs) were made using waste H_2S derived from another process that precipitates metals from mine wastewaters. Biogenic ZnS NPs behaved identically to ZnS quantum dots with absorbance and emission maxima of 290 nm (UVB, which is mostly absorbed by the atmosphere) and 410 nm, respectively; the optimal wavelength for chlorophyll a is 430 nm. By using a low concentration of citrate (10 mM) during ZnS synthesis, the excitation wavelength was redshifted to 315 nm (into the UVA, 85% of which reaches the earth's surface) with an emission peak of 425 nm, i.e., appropriate for photosynthesis. The potential for use in large scale photobioreactors is discussed in the light of current PBR designs, with respect to the need for durable UV-transmitting materials in appropriate QD delivery systems.

Keywords: photosynthetic enhancement, bioenergy, quantum dots, zinc sulfide, *Botryococcus braunii*, *Arthrospira platensis*, *Rhodobacter sphaeroides*, bio-oil, bio-hydrogen, biomass

INTECH
open science | open minds

© 2018 The Author(s). Licensee InTech. This chapter is distributed under the terms of the Creative Commons Attribution License (http://creativecommons.org/licenses/by/3.0), which permits unrestricted use, distribution, and reproduction in any medium, provided the original work is properly cited.

1. Introduction

1.1. Photosynthetic biotechnologies for biomass and fuels

The term "bioenergy" is used to describe the conversion of materials of biological origin into fuels and also includes the use of living organisms to produce a material that is a fuel or fuel precursor. This chapter focuses on the use of photosynthetic microorganisms: bacteria, cyanobacteria, and algae. These all grow at the expense of sunlight, while at the same time fixing carbon dioxide from the atmosphere or dissolved in water (algae) or converting organic waste into biomass material (bacteria). Traditional photobiotechnologies have used algae which range from seaweeds to small unicellular organisms within the "kingdom" of eukaryotes which also includes all higher forms of life. The "kingdom" of prokaryotes represents a far simpler level of cellular organization and includes single-celled photosynthetic bacteria and also filamentous microorganisms called cyanobacteria (or "blue green algae"). This review will illustrate examples of all three types.

Photosynthesis is achieved via the use of specialized pigments called chlorophylls that trap light energy for conversion into chemical energy to drive microbial processes and growth. Algae and cyanobacteria contain "chlorophyll a," while algae, like higher plants, also have a second chlorophyll, "chlorophyll b." Photosynthetic bacteria have functionally equivalent pigments called bacteriochlorophylls, and also ancillary pigments involved in light trapping.

Photosynthetic microorganisms are united by the need to maximize solar irradiation onto their light trapping centers. Natural growth occurs in, for example, ponds but, focusing on maximizing productivity, biotechnology has developed various strategies using photobioreactors (PBRs) for process intensification. Typical strategies include various PBR formats for optimal growth and production at scale, molecular engineering of light trapping centers to improve light conversion and strategies to convert the unused portions of sunlight into additional light which forms the focus of this chapter. Examples will be presented as a proof of concept, highlighting some of the barriers towards implementation.

1.2. Examples of photosynthetic biotechnologies: three examples

By 2030, the global demand for transport fuel is likely to increase significantly, requiring the production of up to approximately 400–500 billion liters of biofuel per year [1, 2]. Biofuel production could rise to 165 billion liters by 2030, if the US, Canada, and Europe adopt a common E15 blending standard [3], but clearly there will be a shortfall. Biofuel production by photosynthetic microbes is an alternative to crop-based biofuels as fertile soil and a hospitable climate are not required, and hence, biofuels could be produced using contaminated land, steeply sloping hillsides, deserts, urban areas, or rooftops. Therefore, unlike crop-based biofuels, microbial biofuels would not necessarily impact upon agricultural food production.

The microscopic alga *Botryococcus braunii* is potentially valuable as it secretes long-chain ($C_{20–40}$) hydrocarbons which can be processed into "drop-in" liquid fuels [1, 4]. As an alternative approach, algae have been grown as a source of biomass for production of another form of bio-oil. Thermochemical treatment (pyrolysis) produces oil, which is akin to fossil oils when suitably processed via upgrading and refinery processes [5].

Cyanobacteria (historically misnamed "blue-green algae") are functionally similar to algae but distinct in many ways. The filamentous cyanobacterium *Arthrospira* ("spirulina") *platensis* is grown as a high-value food supplement and also (under less stringent production standards) as animal feed due to its high content of protein and other nutrients [6, 7]. Spirulina production is highly practical, as the alkaline medium it prefers suppresses contaminants that can impact on algae production. Notably, too, it can utilize soluble bicarbonate ion which forms in alkaline solution, following the dissolving of gaseous CO_2.

The anoxygenic photosynthetic "purple nonsulfur bacteria" (e.g., *Rhodobacter sphaeroides*) offer potentially both fuels and chemicals, producing C_4-C_5 polyhydroxyalkanoates (bioplastic precursors; 50–80% w/w) [8] and high-purity hydrogen gas (typically 90% v/v) as part of an integrated biohydrogen refinery, which could exceed the delivered energy densities of mainstream renewable energy systems, such as photovoltaic cells and on-shore wind turbines [9, 10]. Unlike cyanobacteria and higher algae, *R sphaeroides* utilizes organic acids which are almost ubiquitously produced as by-products from various fermentations and wastewater treatment processes.

Lacking complex structures, microbes can achieve much higher productivity than crop plants. The efficiencies of light conversion to fuel are 0.4–0.8% for algal oil and ~1–5% for purple bacterial H_2 [11], whereas for higher plants, the value is at most 0.16% and normally much less [12]. Significantly higher photosynthetic productivities are needed to make significant progress toward supplanting fossil fuels. As well as improving the microorganism, the "value" of sunlight and its delivery can also be improved, which forms the focus of this chapter.

2. Overview of photobiotechnologies

Bacterial photobiotechnologies are not yet developed at scale, and in some cases, as for the biohydrogen process noted above, the photobioreactor design can be complex due to the need to exclude air. In contrast, algal biotechnology is relatively well developed [13], even though predictable algal culture at industrial scales (10^5–10^6 l), for extended periods, remains problematic [14].

Although the basic requirements for algal culture are simple—water, dilute inorganic nutrients (nitrate, phosphate and trace elements), CO_2, and light—a number of physical and biological factors limit the basic engineering designs of algal culture platforms which, as a consequence, have changed little in the last 50 years. These limiting factors include mainly light attenuation in water (notably of the photosynthetic, red wavelengths) due to absorbance and scattering, CO_2 dissolution, water temperature, and, often overlooked, the fact that algal cultures typically comprise unicellular organisms that are fundamentally "selfish" and are in a permanent competition with all other individuals in the culture [15]. This latter point means that algae are superbly adapted to acquiring more photons than are actually required for their photosynthetic processes and dissipate the surplus as nonphotosynthetic radiation. In algal cultures, illumination typically follows the Beer-Lambert law, with light intensity decreasing exponentially depending on the biomass concentration [16]. Consequently, in static cultures, cells at the surface of the photic zone experience high intensities of light and temperature, while the majority of the culture is in complete darkness [17–19], the consequence of which is that static cultures rapidly become light limited, and overall growth slows or reaches a plateau.

Engineering solutions to these problems typically include: constructing short light paths within the culture system or using high-intensity illumination; mixing cultures using pumps, impellers, paddle-wheels, or bubbles to maintain an overall average illumination experienced by all cells in the culture; controlling temperature; and increasing the concentration of dissolved CO_2. Fundamentally, engineering algal culture systems is a complex problem [20], involving multiple possibilities, and compromises that must be aligned with the final application, as any solution invariably has a cost that will be reflected in that of the product.

Algal culture platforms are conventionally divided into two categories, open or closed systems, each of which has different advantages, uses, and productivities.

Open algal cultures (**Figure 1a** and **b**) are typically shallow ponds, or "raceways", in which mixing is performed by direct displacement of the liquid using impellers or paddle wheels or by bubbles in airlift systems [14]. Raceways are designed to provide predictable, circulatory patterns (**Figure 1c**), enabling a more or less homogenous distribution of nutrients and access to light for all individual algal cells [22]. Although photosynthetically active radiation may not penetrate dense cultures, a combination of shallow ponds (20–50 cm deep) and mixing allows the algae sufficient time in the photic zone to grow (**Figure 1d**). The larger the installation, the more energy is required for mixing, increasing hydrodynamic shear, and the possibility of localized "dead-zones," where mixing is sub-optimal, and resulting in sub-optimal productivities [23]. Moreover, open ponds require large expanses of flat land which, in certain locations, is sought after for other, more lucrative uses, thereby increasing the capital cost of the installation. The addition of CO_2 to open systems is also problematic. Finally, open ponds carry the possibility of culture contamination by undesirable organisms such as other algal species or algal predators. While some applications, notably bioremediation, might benefit from a diverse population of different algal species with regard to resilience, stability, and performance [24–26], when the culture of a single algal species is preferred in an open setting, a limited number of extremophiles and rapidly growing algal species are used to minimize contamination [27].

Closed systems (also termed "photobioreactors" or PBRs), in which there is no direct exchange of culture media, gases, and potential contaminants with the environment, offer a number of advantages for algal culture, including better control over culture conditions (light intensity, temperature, pH, oxygen concentration, and CO_2), higher levels of reproducibility, higher biomass productivity, a lower risk of contamination, enabling culture of a wider variety of species, and, because they are contained, the use of genetically modified algal strains. Several types of PBRs have been devised [28, 29] (**Figure 2**) that can be located either outdoors or, for more accurate temperature control, in greenhouses or in artificially lit chambers. Apart from shaken flasks in an illuminated incubator, the simplest PBR design is a hanging, translucent, or transparent plastic bag or vertical, transparent tube, in which algal cultures are mixed by gas sparging ("bubble columns" or "airlift columns"). Such PBRs have a high surface area to volume ratio suitable for light transmission and satisfactory heat and mass transfer, providing a homogenous culture environment and efficient release of gases. Other advantages include low shear; the lack of moving parts makes bubble columns relatively inexpensive and easy to maintain. Alternatively, algal and media mixing may be achieved by an impeller (so-called "stir-tank" reactors; conceptually similar to an illuminated bacterial fermenter); here, the effectiveness of mixing depends upon the design of the impeller blades, the speed of rotation,

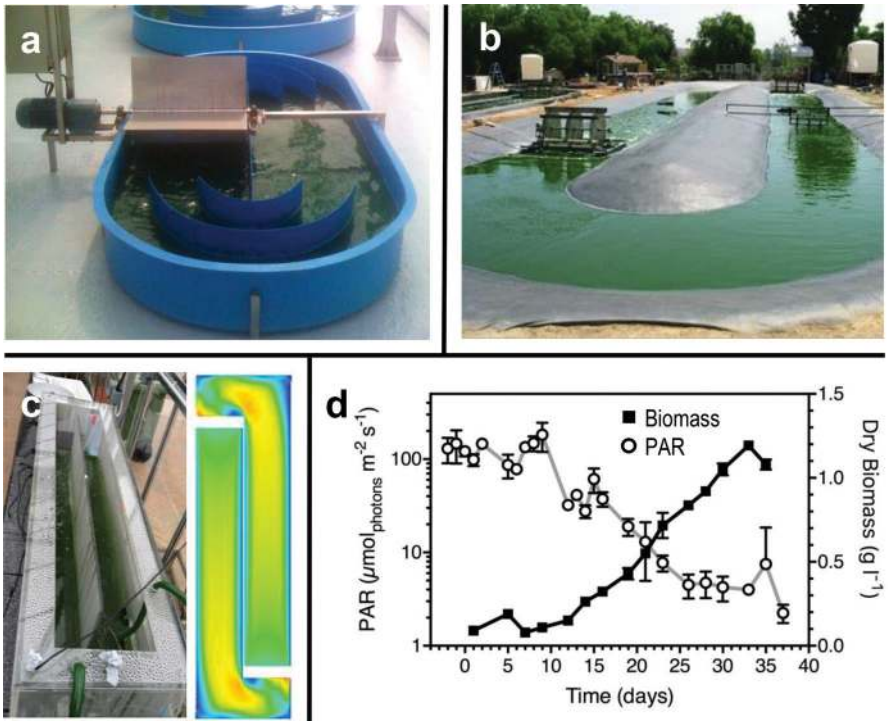

Figure 1. Open algal culture systems. Open-pond systems used for (a) small-scale (≈1000 l) and (b) commercial scale (>100,000 l) algal culture (image courtesy of the South Australian Research Institute (SARDI)), where the medium is displaced by paddle-wheels that are easy to service and cause low hydrodynamic shear. Panel (c) shows a model raceway (200 × 50 and 20 cm water depth) in which currents are driven by impellers. Computational fluid dynamic (CFD) modeling of this system topography (panel c, right) shows the distribution and strength of currents, with regions of low water movement in cold colors and faster water movement represented by warmer colors. The CFD was performed by Robert Rouse and Gavin Tabor (University of Exeter Department of Engineering) using empirical data. The graph in (d) shows the growth of a *Botryococcus braunii* culture (closed squares representing the mean of 3 replicates) in a 20 cm deep raceway and the reduction in photosynthetically active radiation (PAR; open circles representing the mean of readings from 4 sensors placed under the tank and 49 cm intervals) at the bottom of the pond, as the culture grows. Note that after approximately 15 days, PAR is only 10% of the starting level but, due to mixing, the culture continues to grow for a further fortnight. Bars represent the standard error of the mean.

and the depth of liquid. Vertical or horizontal tubular reactors in which media and algae are pumped from a main sump through the structure ("biofence") provide a scale-up capacity to several hundred liters. Shorter light paths are achieved using flat-panel reactor designs.

Illuminating plants with light emitting diodes (LEDs) leads to higher biomass productivity per unit of irradiance [30]. LEDs have several advantages over conventional, incandescent, or fluorescent lights, including small size, durability, long lifetime, cool-emitting temperature, and the option to select specific wavelengths, notably in the photosynthetic red and blue wavelengths [31, 32].

Despite the concomitant reduction in energy use from LEDs compared to other forms of illumination, and the effectiveness of different PBRs at laboratory scale, the mass production of

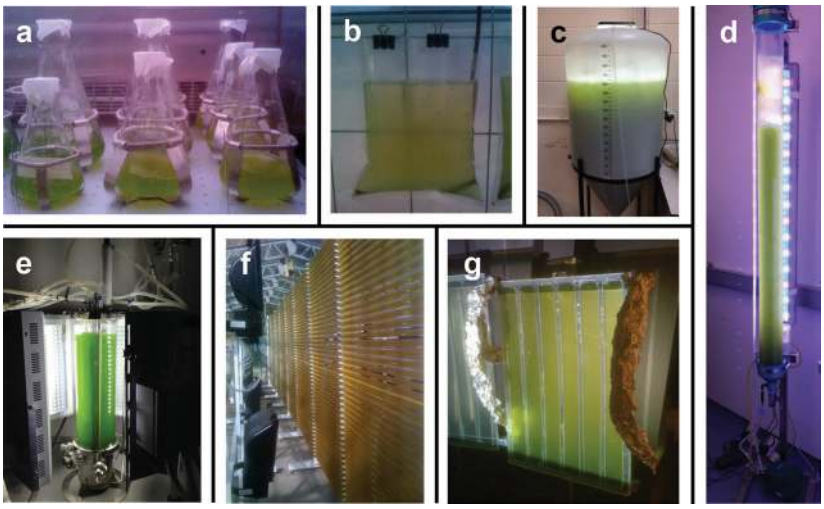

Figure 2. Examples of closed algal culture systems. (a) Flasks containing 100 ml of algal culture in a shaking, lighted incubator with CO_2-enriched atmosphere. (b) Polyethylene bag containing 100 ml of algal culture, located in a greenhouse with natural and complementary artificial lighting. Mixing is achieved by an air-stone (aquarium) bubbler. (c) Translucent polyethylene, conical bucket for airlift culture, containing 100 l for media. Air is provided by a simple tube at the bottom of the vessel. The conical shape and tap towards the bottom of the container enable simple harvest of the algal suspension. Photograph courtesy of Dr. Mike Allen, Plymouth Marine Laboratory. (d) Airlift column photo-bioreactor (perspex; 2 m in length; 10 cm in diameter), containing 10 l of culture and lit by a combination of white, blue and red LED's optimized for algal growth. An air inlet at the base of the column provides mixing. (e) Stirred photo-bioreactor with white LED light jacket, containing 2 l of algal culture. (f) Horizontal, tubular photo-bioreactor (or "biofence") containing 600 l of *Phaeodactylum* culture, located at Swansea University (Wales, UK). The culture is pumped through the transparent tubes from a sump enabling control of media composition and temperature. (g) Flat-panel photobioreactor containing 100 ml of algal culture. The light path is 5 mm and the algae are pumped through the reactor from a sump.

microalgae in closed systems remains expensive in terms of construction costs, materials, and energy. Moreover, up-scaling is problematic, as most PBR designs suffer from a number of limiting factors, including poor gas exchange, difficulties in nutrient delivery, heat balance, and, in locations where seasons are marked, available light [33, 34].

3. Process intensification: Limitations of light availability

The problems of light delivery to a photobioreactor are 2-fold. In equatorial regions, the photoperiod (day length) and seasonality are reasonably constant. However, at higher and lower latitudes, the day length and incident light are seasonally variable, and hence, for a proportion of the year, a PBR cannot operate during significant periods of darkness or is impaired by low light intensity. A pilot scale tubular photobioreactor using *R. sphaeroides* to produce hydrogen (**Figure 3a**) was programmed to operate at UK latitude (~55°N) at equinox and maintained on that diurnal cycle for 3 months, with the light intensity varied day to day. Saturation occurred at ~400 W/m^2 (**Figure 3c**). **Figure 3d** shows that in spring and autumn, a

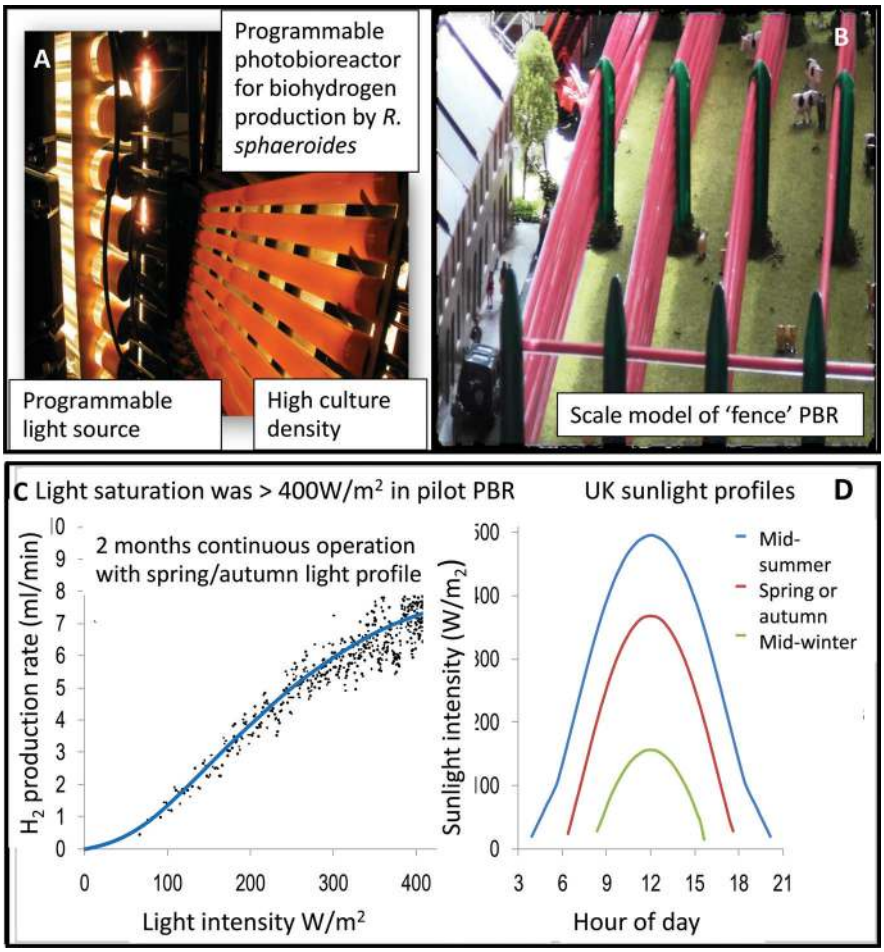

Figure 3. Performance of a programmable photobioreactor. The PBR was operated over 3 months of continuous diurnal operation set to spring and autumn equinox (12 hour days/nights plus dawn/dusk periods). The light intensity was varied from day to day (at random) and parallel rooftop tests confirmed the pilot scale data. A. PBR tubular construction and orange-pigmented *R. sphaeroides*. B. Scale model of full scale PBR constructed on the basis of the pilot data C: Determination of light saturation in terms of biohydrogen productivity. D: Light intensity (W/m^2) as typical UK profiles.

PBR will not reach light saturation, while in winter, the productivity would reach only ~33% of its potential maximum at midday (**Figure 3c**, **d**). Saturation would only be reached in mid-summer (**Figure 3d**); hence, an increase in light intensity of up to 4-fold would be required for maximum productivity.

To attempt to overcome the limitation, the culture biomass intensity/ml can be increased, but this results in significant "self-shading". In illustration, using the spring/autumn illumination profile (**Figure 3c**) of the biohydrogen PBR using low, intermediate and high density cultures gave a hydrogen yield of 11.5, 7.0, and 3.5 ml/min, respectively, i.e., simply introducing more bacteria is

counterproductive, and this also increases the running costs with respect to both the make-up feed (trace nutrients) and the final biomass for waste disposal, if the biomass is not used for biofuel.

The second limitation is that the solar spectrum is very wide, yet the wavelengths captured by photosynthetic pigments are quite conservative (**Figure 4**), with algal/cyanobacterial chlorophyll utilizing visible wavelengths, while bacteriochlorophyll utilizes light in the visible/near infrared (NIR) region.

A novel study used a beam splitting approach to supply an algal and a bacterial system (similar to that shown in **Figures 5** and **6**, without quantum dots), taking advantage of their respective preferred wavelengths and giving the potential to operate two parallel PBRs. This enhanced the microbial productivity per incident photon [35], an approach that could be useful in, for example, biohydrogen production, where bacteria and algae both make bio-H_2 but by using different pathways [36]. Hence, it may be possible to produce bio-H_2 by bacterial and algal reactors side by side, with the additional advantage of providing a "sink" for bacterially produced CO_2 into algal biomass.

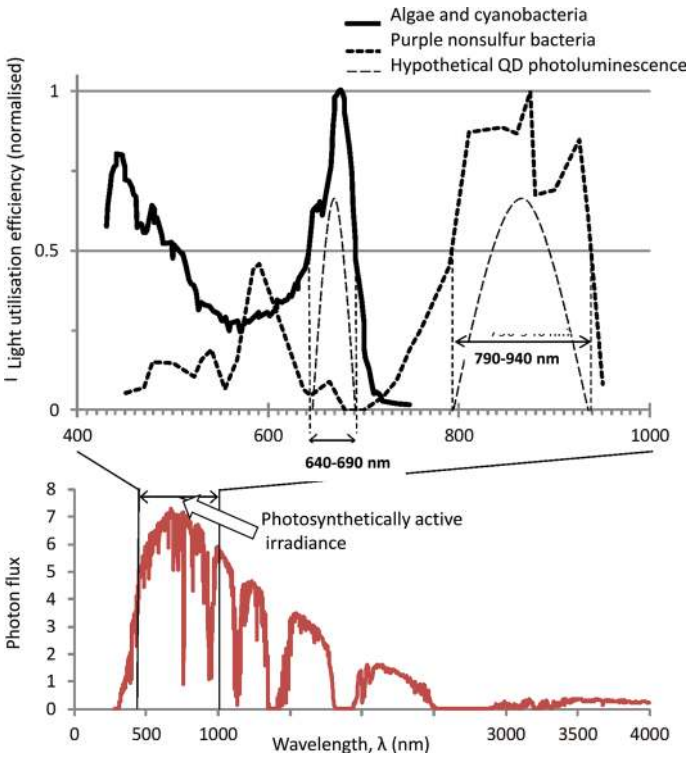

Figure 4. Action spectra and identification of targets for spectral enrichment. Generic action spectra were adapted from [35]. Note that action spectra differ substantially from whole-cell absorption spectra, which show strong wavelength-nonspecific attenuation due to the scattering effect of cells. Above this, small peaks associated with the absorption maxima of chlorophylls can usually be detected. The emission of the desired quantum dots is shown by the dotted line; ideally the emission peak should be narrow and overlap with the absorption maxima of the algal and bacterial chlorophylls.

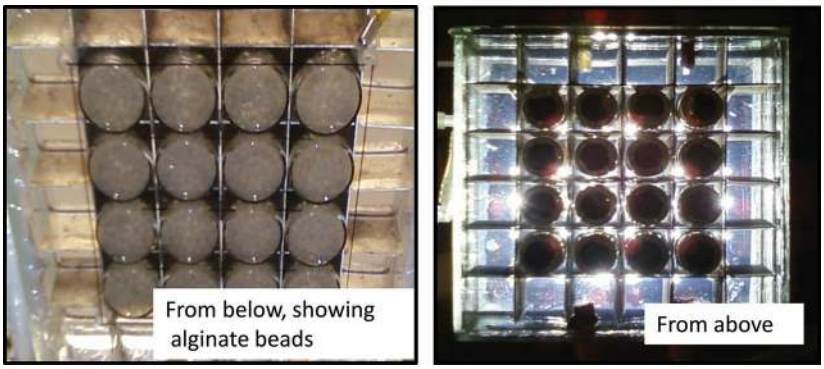

Figure 5. Boosting photosynthetic activity of *Rhodobacter sphaeroides*. Qdot'792 (to 20 nm) was encapsulated in 2% alginate beads (diam. 2.6 ±0.04 mm). Beads were prepared by mixing QD or blank (50 mM sodium borate buffer, pH 9.0) with 2% sodium alginate and dropping into 100 mM $CaCl_2$ through an 18G needle. After curing (60 min), the beads were washed with deionized water and used immediately. Concentrated cell suspension was diluted to 0.547 gdry weight/l with fresh butyrate medium [35]. Vials (4 ml bacterial suspension, 3 ml beads containing Qdot'792 and ~5 ml headspace) were sealed with gastight stoppers and purged with argon (30 min in darkness) and incubated (30°C, 3d, 10.0W/m^2 simulated sunlight). H_2 formation was measured as described previously [35]. Each vial contained 0.056 nmol Qdot'792 distributed over an illuminated surface of 3.14 cm^2. Optical dividers prevented optical interactions between vials and ambient light was excluded by covering the assembly with black cloth.

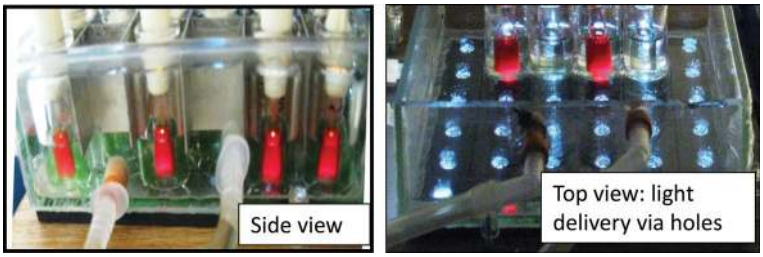

Figure 6. Boosting photosynthetic activity of *Arthrospira* ("spirulina") *platensis*. Growth was as in [35]. Inocula for photonic enhancement experiments were taken 2 days after subculturing (to ensure active growth) and diluted with fresh medium to an OD 660 of 0.364.4 ml was transferred into each vial. Cultures were illuminated by a close-match solar simulator undergrowth-limiting irradiance (10W/m^2) (supplementary material in [35]. Photosynthetic action was inferred from growth measured after 22 h [35]. To isolate optical effects, QDs were isolated in a glass insert, each containing 1 ml of Qdot'652 in 100 mM Na_2SO_3 with controls of QD-free Na_2SO_3. The inserts aligned with 10 mm openings in an opaque sheet to allow illumination from beneath with artificial sunlight. Ambient light was excluded by covering the assembly with black velvet and opaque barriers were placed around each mini-reactor. The temperature was controlled by circulating water at 30°C.

However, in practice, other than to make a common product in an integrated process, it may be impractical to co-locate both types of PBR due to other requirements; for example, organic acid feedstock for bacterial hydrogen production can be supplied by urban wastewater treatment plants [37], whereas algal biotechnologies typically require a large land area which can be waste or nonarable land. Hence, a generic method is required to "upgrade" solar light by converting unused wavelengths into used wavelengths for a particular process, thereby increasing the usable light and productivity without increasing biomass density and "self-shading". This forms a goal for photobiotechnology process intensification.

The wavelength dependence of photosynthesis by purple bacteria and microalgae has been known since the early twentieth century and confirmed many times in different species. As shown in **Figure 4**, green algae/cyanobacteria/higher plants show the greatest activity with red light, whereas purple bacteria are most active under near-infrared (NIR) [38–42]. The effect is so powerful that these organisms have developed an apparent "phototaxis" response, accumulating in the optically optimal part of a natural water column [38]. This ability is very important because red light is absorbed strongly by water, and hence, the availability of useful light drops markedly with depth. Blue light has a far greater penetration (see later).

The action spectra of photosynthetic microorganisms have been extensively surveyed. Green microorganisms (and plant chloroplasts) conform to a generic action spectrum, while purple bacteria conform to a distinctly different generic action spectrum (see [35] and **Figure 4**) attributable to the different chlorophylls evolved in the taxanomic groups.

4. Quantum dots as a potential means of "upgrading" light

One method of "upgrading" "waste" light of a particular wavelength is to use the light-emitting properties of quantum dots (QDs). QDs are single crystals of uniform size and shape of ~2–10 nm diameter and usually comprising pairs of semiconductors (e.g., CdSe, PbSe). QDs are replacing fluor dyes in cell biology due to their high brightness and photostability [43]. The properties and potential applications of QDs are described elsewhere in this volume, and indeed, QDs are commercially available in appropriate delivery systems for boosting horticulture and small-scale crop production [44] but have yet to find application in large-scale photobioreactor systems. However, for bioenergy applications and bulk-scale animal feed production, large scale constructions would be required (e.g., see **Figure 3b** and **Table 1**). Hence, a feasibility study was undertaken using the three microorganisms described above to indicate whether photosynthetic boosting via QDs is feasible for algal and bacterial growth systems. The use of LEDs to supply additional lighting at the optimal wavelengths is well-established technology [44, 45], and it is assumed to be intrinsically scalable, although a full cost-benefit analysis is required for applications in biofuels production.

4.1. Boosting of three photosystems using quantum dots

The concept of photonic enhancement is to increase the proportion of the solar spectrum that corresponds to the major peak(s) of the organismal action spectrum (**Figure 4**), at the expense of other irradiance at less active wavelengths. The part of the spectrum to be intensified is referred to as the target band. **Figure 4** (top panel) shows the boundaries of the target band corresponding to the half maximum of the major peak in the organismal action spectrum. Using generic action spectra derived previously [43], the target bands of 640–690 nm and 790–940 nm were determined for algae/cyanobacteria and purple bacteria, respectively. These bands account for 25 and 67% of the total action, respectively.

The study used test quantum dots purchased from Invitrogen: Qdot'792 (ITK carboxyl, no Q21371, lot 834,674; quantum yield (QY) 72%; full width height maximum (FWHM): 82 nm) and QD'652 (ITK carboxyl, no. Q21321MP, lot 891,174; QY 78%; FWHM 26 nm) for cultures of *R. sphaeroides*

PBR type	Dimensions; vol, m^3	Algae production kg dry solids/yr	Microalgae cost price (€/kg dry solids)	Ratio electricity*/variable cost# (%)
Open pond	1000 m^2; 0.03 m water depth; 300 m^3	1538	36	35
Tubular	1000 m^2; 0.06 m tube diam.; 45 m^3	3076	18	50
Flat panel	1000 m^2; 0.03 m plate spacing; 60 m^3	5127	12.50	68
Solar LEDs/flat panel*	1000 m^2; 0.03 m plate spacing: 60 m^3	12,818*	~ 4.20*	~30*

*Electricity is taken from the grid (@ €0.107/kWh) and includes "parasitic energy" consumption (pumps for culture and water heating/cooling circulation, centrifuge and blower for the flue gas supplying CO_2).

#Projection via use of solar cells, efficient battery technology and LED supplementary illumination. Calculations by R.L. Orozco (unpublished work).

#variable cost includes cost of water use, electricity (parasitic energy), labor, fertilizers (N & P) and waste water. V: culture volume.

Table 1. A comparative study [21] on algal (***Chlorella vulgaris***) cultivation technologies which include open pond and closed photobioreactors (PBRs: Tubular and flat panels) and economics of algal biomass production. The high productivities of flat panels compared to the other systems are reflected in the lower cost price.

and the cyanobacterium/green alga spirulina and *B. braunii,* respectively. The loading densities in the tests were 0.0178 (*R. sphaeroides*), 0.0792 (spirulina), and 0.050 (*B.braunii*) nmol/cm^2.

4.2. Experimental test systems

4.2.1. Rhodobacter sphaeroides for biohydrogen production

R. sphaeroides was used in a test system of mounted vials as shown in **Figure 5**, using simulated sunlight.

4.2.2. Spirulina for biomass production

Arthrospira platensis (spirulina) was used in a test system (**Figure 6**) using a close-match solar simulator (supplementary material in Redwood et al. [35]).

4.2.3. B. braunii: A single-celled alga for bio-oil production

B. braunii was cultured routinely in shake flask cultures. Q dot'652 was added directly into small 25 ml cultures to 10 nm. Cultures were shaken in a temperature-controlled greenhouse (average solar photon flux was 11 μmol/m^2/s). Photosynthetic action was inferred from growth at 21 days as estimated by OD_{600}.

4.3. Photosynthetic enhancement using commercial quantum dots

The first test, using *R. sphaeroides* to produce H_2, showed a photonic enhancement of ~10% (**Table 2**; **Figure 8c**). This was a close fit to the increase predicted by the known QD quantum efficiency

and the QD loading/cm^2. Photonic enhancement of the growth of *A. platensis* (spirulina) doubled the biomass yield, which was ~25% higher than a predicted stimulation on the basis of quantum yield and QD loading density (**Figure 8d**). In this example, the QDs were held separate from the culture (**Figure 6**), which rules out stimulation via components leaching from the QD preparation. Finally, using *B. braunii* with QDs added directly into the culture and incubated in sunlight, the biomass yield was increased by 2.4-fold (**Figure 8b**). This photonic enhancement, 2.4-fold with respect to optical density, was >50% higher than that predicted on the basis of quantum yield and loading. A growth stimulatory effect of contaminants was largely ruled out on the basis of the test using spirulina, which was held separate from the cells (above). However, as *B. braunii* becomes heavily loaded with oil globules during growth (**Figure 7**), their contribution to increasing the size (and hence OD_{600}) of the cells cannot be precluded. The effect of photosynthetic enhancement on oil production was not examined in this study. It was concluded that the use of QDs as photonic enhancers has potential, but the light emission from the commercial QDs was not at the ideal wavelength (**Figure 4**), while the high cost of commercial QDs would currently be prohibitive in large scale systems, although the potential cost reduction at bulk scale is not known.

Microbial group	Organism	QD-free controls	Experiment with QDs*	Photonic enhancement*
Purple nonsulfur bacteria	*Rhodobacter sphaeroides*	15.54 ± 0.31 (13)	17.00 ± 0.16 (13)	1.1-fold
Cyanobacteria	*A. platensis*	0.025 ± 0.002 (6)	0.052 ± 0.011 (4)	2.1-fold
True algae#	*B. braunii*	0.106 ± 0.032 (3)	0.251 ± 0.011 (3)	2.4-fold

Data are means ± SEM for the number of experiments shown in parentheses. Photonic enhancements are modest due to the low dose of QDs used but were in accordance with theoretical predictions. The maximum enhancement was not tested. Enhancements are statistically significant at P = 0.95.

*The criterion for the algae was biomass content/ml (OD_{600}) that for *R. sphaeroides* was production of hydrogen.

#Data from shake flask tests.

Table 2. Photosynthetic boosting using quantum dots.

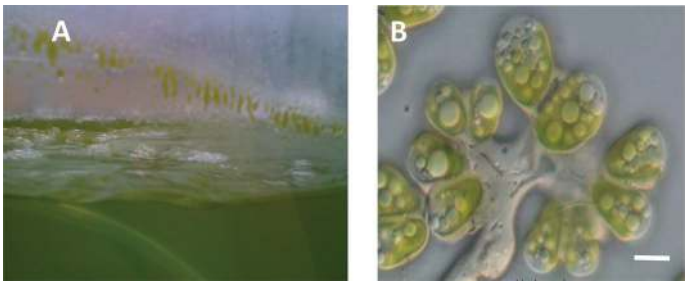

Figure 7. *Botryococcus braunii*. (A) Twenty-day-old *Botryococcus braunii* culture in uplift photobioreactor. (B) Bright field image of *Botryococcus braunii*, Race B. Pyriform *B. braunii* cells held together by a hydrocarbon-polysaccharide matrix. Oil containing vesicles are clearly visible inside the cells, which contain a single chloroplast. Images were acquired using an Olympus BX51 System Microscope with an attached DP71 digital CCD camera. Image processing and analysis software used was Cell F version 2.8 from Olympus).The scalebar represents 5 μm.

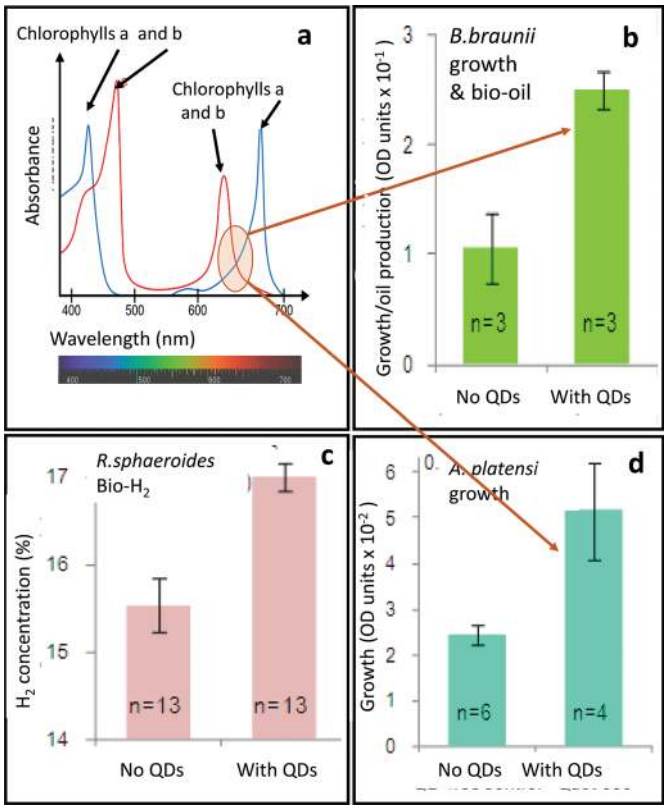

Figure 8. Enhancement of photosynthetic activity using QDs in three test systems. (a) Spectrum showing absorbance of chlorophylls a and b, and QD emission. Red emission was used (circled) for the algae and near infra red emission for *R. sphaeroides* (not shown). (b), (d) Photoproductivity of *B. braunii* (b) and *A. platensis* (d) with QDs (c) Hydrogen production by *R. sphaeroides* with QDs. N is the number of tests in each case.

5. Factors affecting development of quantum dots for enhancement of photosynthetic biomass and biofuel processes

This feasibility study (carried out in 2012) was limited by the suitable but nonideal properties of commercially available QDs. Small shifts in the emission peaks could improve the photonic enhancement, particularly in purple bacteria.

For cyanobacteria and algae, the available Qdot'652 was suitable as the major peak in the action spectra of cyanobacteria and algae occurs inside 640–690 nm (**Figure 4**), while the main part of the emission of Qdot'652 was within 639–665 nm (boundaries placed at half-maximum). Further development would aim to adjust the emission peak to ~655 nm while maintaining high quantum yield (QY) and full width height maximum (FWHM) ≤35 nm. For purple bacteria, the major peak in the action spectrum occurs inside the 790–940 nm region (**Figure 4**), while the main part of the emission of Qdot'792 was within 751–833 nm (boundaries placed at

half-maximum). Therefore, a significant fraction of the emission fell outside the target band. Further development using this method would aim to adjust the emission peak to ~855 nm while maintaining high QY and FWHM ≤83 nm, thereby placing almost all QD emissions within the target band. For cyanobacteria and algae, this would require a FWHM for the QD of ≤35 nm, which matches the manufacturer specifications for Qdot'655. However, for purple bacteria, this could be more challenging as the longer wavelength emitting QDs typically produce broader emission peaks. However, the major action peak for purple bacteria is also broad (770–940 nm; half-maximum; **Figure 4**), suggesting an ideal emission peak of ~855 nm with FWHM ≤83 nm, which is similar to published specifications.

The discussion does not consider other potential impacts of QDs on the photobiological apparatus. The absorbance of less useful solar wavelengths by QDs could protect against damage from heat and UV irradiation, a benefit that would not be apparent from the experiments described here, as the temperature was actively controlled and much of the UV element of sunlight was absorbed by several layers of glass before reaching the QDs or the culture.

In this feasibility study, a single type of QD was selected to align as closely as possible with the major action peak of the organism. Further development could combine different QDs to further enrich the solar spectrum, according to the minor action peaks (**Figure 4**). There is also further potential in using combinations to further enrich the spectrum at ~680 or ~850 nm above the model presented here. Nature has evolved complex but optimal systems, for example, purple bacteria have ancillary pigments which absorb light in the visible region (e.g., 400–500 nm) and transfer energy very rapidly onto the bacteriochlorophylls [46, 47]. A biomimicry approach could use alternative QDs to construct a spectrum that precisely mirrors the action spectrum.

One important technical factor affecting practical photonic enhancement would be the stability of QDs. QDs can be affected by photobleaching [48], and the leaching of QD degradation products could have a potential negative environmental impact. Therefore, further investigations should focus on QD immobilization methods, aiming to make QDs a permanently encapsulated part of a photobiological installation and to enable low-risk handling in large quantities and recovery for multiple uses.

Finally, since the photobiotechnologies envisaged here would necessarily be at large scale to supply energy carriers for replacement fuels (as compared to the relatively small PBRs used for high-value products), maximum light transfer from sunlight to the QDs and light upgrading to the cells is essential, while maintaining a minimum QD loading for economy.

Color	Wavelength, nm	Percentage absorbed in 1 m of water (%)
Violet	400	4.2
Blue	475	1.8
Green	525	4.0
Yellow	575	8.7
Orange	600	16.7
Red	725	71.0
Infrared	800	82.0

Adapted from [49]

Table 3. Light attenuation in water.

However, given poor penetration of the red component of sunlight in water (**Table 3**), it is apparent that a deep QD-reactor system with irradiation from above would be unsuitable for purple bacteria as they use red-infrared light. An algal system is less sensitive to culture depth, as it can utilize blue light; the loss of light at 655 nm was calculated to be ~30%, which would still be a factor to consider in photobioreactor design. However in the blue region, corresponding to an absorption maximum of chlorophyll b (575 nm: **Figure 4**), very little light is lost, while at 430 nm (optimum for chlorophyll a), the available light intensity is still acceptable with depth, meaning that "point" sources of QD light could be used (insets or roof panels).

6. Potential alternative strategy for economic production of quantum dots at scale

For incorporating quantum dots into photosynthesizing cultures, some forms of QD encapsulation or barrier method are likely to be required (see above), while the use of toxic materials *per se* is unattractive for manufacturing, even assuming that the QDs are held separate from the cells, are easily recovered and are re-usable. Given the high cost of commercial quantum dots, the possibility to use more traditional metallic-based semiconductors was revisited, since these can be made economically at scale, but the use of highly toxic metals such as Cd should still be avoided. The waste hydrogen sulfide off-gas from an (unrelated) bioremediation process was considered for use to promote the formation of zinc sulfide nanoparticles which are well-known QDs. Using a waste from a remediation process (which is, in itself, used to recover Zn and Cu from acidic mine wastes [50, 51]) is a paradigm example toward realizing a circular economy. The liquid minewater wastes are obtained via the activity of microorganisms that leach the metals out of ore residues and closed mines. They also lower the pH (by formation of sulfuric acid), and hence, they are acid-loving bacteria (acidophiles). The acidophilic bacteria are fed by using additional nutrients derived from an algal source, *Coccomyxa onubensis,* and hence, development of a method for enhancing growth of this alga via a QD-enhancement approach would impact positively on the economics of the primary metal recovery process (combined metal bioleaching and recovery as metal sulfides), which produces excess waste H_2S from the activity of sulfate-reducing bacteria. These convert sulfate (dilute H_2SO_4) to sulfide, which is available to form ZnS quantum dots by combination with Zn^{2+} ions. This strategy was tested in principle.

Zinc sulfide has a bandgap varying from, in bulk material, 3.7 eV to, in nanoparticles, 4.2 eV [52, 53]. It has large exciton energy (~ 40 meV) and has been used in light-emitting diodes and, for example, flat panel displays [54]. The nanoparticles have to be stabilized during synthesis in order to minimize extensive agglomeration. This is important because the quantum yield is lower in larger particles [54].

Methods of QD nanoparticle synthesis commonly use organic solvent [55], capping agent, and/or surfactant in order to control agglomeration. These methods may introduce problems of reproducibility as well as complexity and cost, as well as leaving residual chemicals and hence being nonsustainable (see [56] for overview). Looking toward large scale manufacturing, various "traditional" methods could reduce the high cost of ZnS NP-synthesis. Khani et al. [57] incorporated 2-mercaptoethanol as a capping agent; Na_2S and mercaptopropionic acid have also been used [58]. Here, refluxing with tetrapropyl ammonium hydroxide resulted in QDs of nanoparticle size 4.5 nm, and the respective absorption and emission peaks were 315

and ~415 nm [58]. Other work reported QDs with absorbance and emission peaks at 279 and 435 nm, respectively; this method utilizes thiolactic acid with Zn^{2+} solution and Na_2S [59]. Being very close to the absorption peak of chlorophyll a at 430 nm (**Figure 4**), this raises the possibility to use ZnS NPs as a quantum dot ancillary to Qdot'655 (above) or, indeed as a substitute for the latter, using emitted blue light via the other absorbance region for chlorophyll a (see above).

A first report [60] showed that the characteristics and the light emitting properties of ZnS quantum dots made by use of bacterially made waste H_2S left over from the metal bioremediation process [50, 51] were comparable to those made by "classical" methods, which required more complex procedures. As a potential synthesis method at scale, this shows potential for commercial QD production and introduces the possibility to use these biogenic ZnS QDs to promote algal growth for the applications described above and also to provide algal feedstock as a nutrient source for other processes (e.g. high-value chemicals); algae as biomass feedstock *per se* for pyrolysis oil production has also been reported (e.g., [5]).

The price of commercial QDs discourages development above small-scale and a full-scale energy plant is probably currently unfeasible. However, QDs are rapidly developing from niche markets into consumer electronics [61], which is expected to bring substantial increases in production scale, and hence, reduction in cost may be expected in the future. From the tests and data shown above, the QD cost would have to be reduced by up to 100-fold in order for photonic photobioreactors to achieve parity with standard PBRs in terms of capital cost (M.D. Redwood, unpublished). This estimation was based on early published values for capital costs of different photobiological systems [62–65] and a survey (in 2012) of market prices for commercial QDs. Because open systems or raceways present much lower capital costs (per unit area) than enclosed PBRs, the estimated minimum QED cost reduction would be ~10 fold more attractive for raceways, suggesting that such enhancement would be first tested in PBRs then developed in raceways at scale as costs fall.

However, these estimations do not consider the reduced land requirement and reduced running costs of photonically enhanced photobioreactors, which may lessen the cost impact. On the other hand, end-of-life decommissioning may be more costly if potentially toxic metals have been used. QD retention via immobilization/encapsulation and re-use would be a key strategy. The extent to which biofouling of transparent surfaces in contact with the culture may impact adversely on QD-enhanced PBR useful life has not been taken into account (nor tested). Common methods to remove biofouling deposits (e.g., scraping) may damage surfaces that have been precision-machined or polished for optical transmission. Hence, an air gap between the QD enclosure and the culture liquid may prove beneficial. In practice, as long as there is sufficient stirring, the shear force is sufficient to prevent fouling problems. This means that sufficient shear force being produced by sparging of the PBRs can prevent the algae being able to settle on the (e.g., perspex) surface. However, if the perspex is scratched, then algae will adhere more readily. In some cases, fouling can be a major problem; some algal species are more adherent than others, but if the circulation in the PBR is sufficiently high, the algae will not adhere. Conversely, if the shear forces are too high, this may damage the algae. Most of the species that are grown commercially are fairly robust, but some species are shear sensitive; hence, this would need to be tested on a case by case basis (D. McKenzie, Xanthella Ltd., personal communication).

Based on this discussion, and the ease and potential scalability of bimanufacture of ZnS quantum dots, these were considered as a possible alternative to boost photosynthetic output

via irradiation of chlorophyll a in the blue region, as an alternative to visible-red wavelengths, also noting the preferred use of blue light for deep culture (above). The emission of biogenic ZnS QDs prepared in 50 mM citrate buffer, pH 6, was reported at 410 nm [60], whereas the optimal absorbance wavelength of chlorophyll a is ~430 nm (**Figure 4**); respective molar extinction coefficients at 410 and 431.66 nm were calculated as 70,733 and 110,789 cm^{-1}/M, respectively [66, 67]. At ~425 nm, this was given as 93,099 and 98,874 cm^{-1}/M at 424.8 and 426.15 nm, respectively [66]. This illustrates the need to redshift the QD emission of the biogenic ZnS QDs by up to 15–20 nm to realize the full potential.

7. Toward realizing useful quantum dots from biogenic ZnS

The early study [60] used 50 mM citrate buffer (pH 6) to prevent uncontrolled precipitation of ZnS by chelating the Zn^{2+} in solution and acting as a passivant for the ZnS nanoparticles.

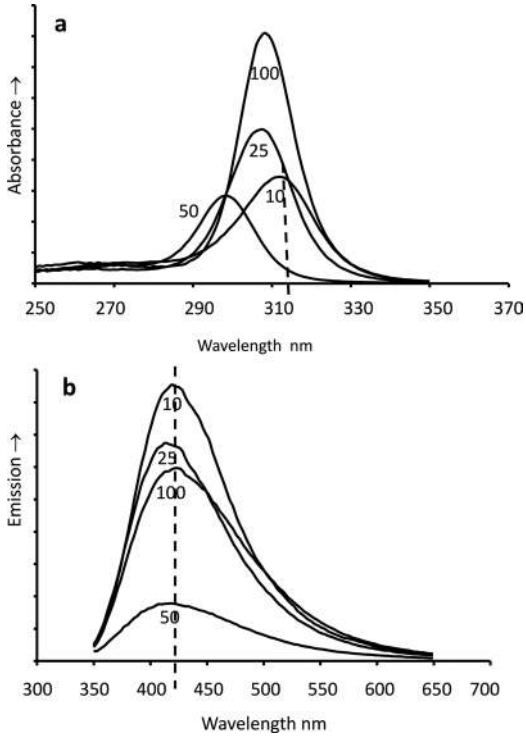

Figure 9. Excitation (a) and Emission (b) Spectra of ZnS Quantum dots. QDs were synthesized using excess waste biogenic H_2S from a metal bioremediation process [60]. Samples were sparged with the culture off-gas for 30 min (flow rate 132 ml/min). Example scans are shown. ZnS QDs were made in the presence of 10 mM, 25 mM, 50 mM and 100 mM citrate buffer (pH 6) as shown. Note excitation redshift to ~ 310 nm and emission from ~ 410 to ~425 nm (dotted lines) with decreased citrate concentration from 50 to 10 mM. Buffering at pH 6 without citrate (MES-NaOH buffer) gave material with negligible emission.

However, the use of citrate should be minimized for process economy. Omission of citrate or its substitution by 50 mM MES-NaOH buffer gave a ZnS nanomaterial with poor light emission at 410 nm. By using lower concentrations of citrate in preparation (10 and 25 mM), the light emission was observed to increase by up to 5-fold, together with a redshift from 410 to

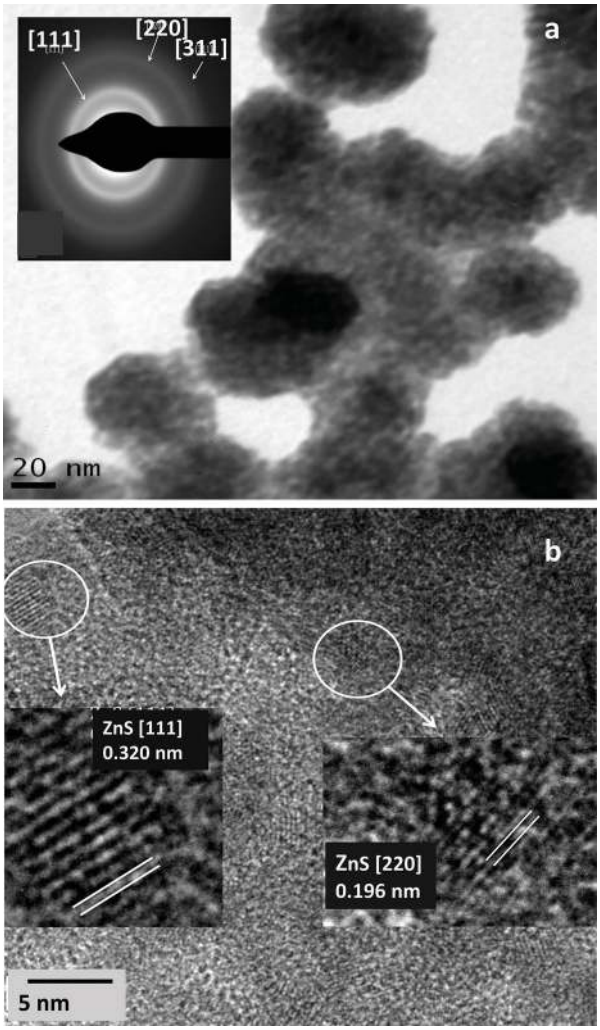

Figure 10. Transmission electron microscopy of ZnS Quantum Dots. QDs were synthesized in 50 mM citrate buffer, pH6 using biogenic H_2S [60]. Accelerating voltage was 80 kV which is optimal for contrast and shows (a) agglomerations of ~60 nm containing discrete small nanoparticles. (b) High-resolution TEM study (300 kV) of a single area of an agglomerations how nina.Lattice details are visible showing facets of ZnS:(111) and (220) corresponding to interplanar spacings of 0.320 nm and 0.196 nm. a (inset): Selected area diffraction of a single nanoparticle at accelerating voltage of 300 kV. The diffraction rings correspond to the (111), (220), and (311) facets of ZnS by reference to the JCPDS database. Calculations from Image J software, in collaboration with J. Gomez-Bolivar.

425 nm, i.e., into the absorption peak for chlorophyll a (**Figure 9**). Increasing the concentration of citrate (to 100 mM) during QD synthesis gave a similar effect; the reason for this was not investigated but future development would require the minimum amount of citrate. Further tests showed that further reduction of the citrate concentration to 7 mM retained the emission peak at 425 nm.

It is well known that increasing the size of quantum dots produces a redshift in the emission spectrum [68]. Hence, the ZnS QD material produced from the biogas from Zn^{2+} solution using high (50 mM) and low (7 mM) concentrations of citrate was examined using two methods: high resolution transmission electron microscopy (HRTEM) and differential centrifugation analysis for determining the size distribution of native nanoparticles.

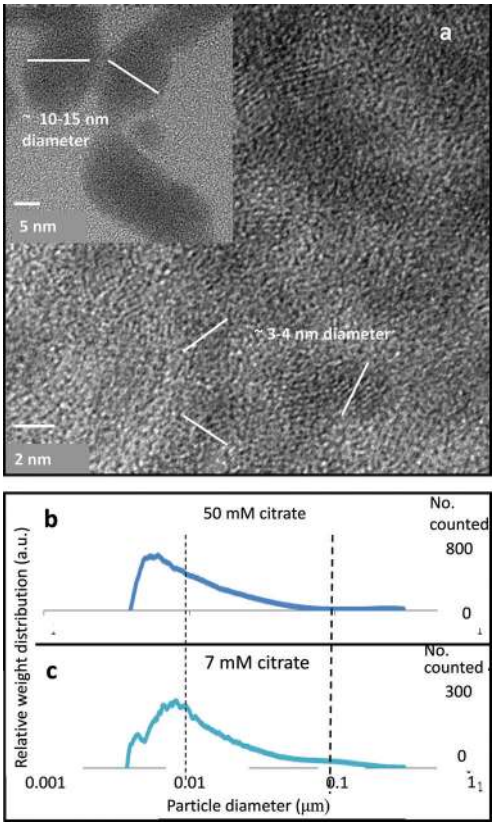

Figure 11. High resolution TEM study and population size analysis of ZnS QDs made under two citrate concentrations. Biogenic H_2S was used to make ZnS in 50 mM citrate buffer (a, main image) and 7 mM citrate buffer (a, inset). Approximate respective nanoparticle sizes are 3–4 and ~ 10 nm as shown. The population from 7 mM citrate solution had additional small nanoparticles of size ~5 nm (a, inset). Bars are 2 and 5 nm as shown. b,c: Estimation of nanoparticle sizes using an analytical disc centrifuge as described in [60] using light scattering. The nanoparticle size in 50 mM citrate buffer was calculated (from log plots) as ~4–5 nm and in 7 mM citrate buffer was ~ 8–10 nm with a smaller population of size <5 nm. The small nanoparticles are too close to the lower size cutoff of the instrument [60] to be an exact measurement, but the two independent methods report the same result. **Figure 11a** was in collaboration with J. Gomez-Bolivar.

Examination of the ZnS material (from 50 mM citrate) revealed agglomerations, within which small NPs were visible [60] (**Figure 10a**). Examination of these confirmed their identity as ZnS (**Figure 10a**, **b**). Use of 7 mM citrate produced larger nanoparticles (**Figure 11a**) consistent with the redshift observation in **Figure 9** (see above). Electron microscopy can produce artifacts due to drying [60]. Hence, independent confirmation was provided via analytical centrifugation of the liquid suspension in conjunction with light scattering (**Figure 11b**, **c**).

Examination of nanoparticle sizes by the two methods gave similar results (**Figure 11**). The nanoparticles made with 7-mM citrate were of size in the region of ~10-12 nm with a subpopulation of small NPs of 5 nm or less. In contrast, when made in the presence of 50 mM citrate, the population comprised small NPs of size 3–5 nm. Accurate sizing of the latter was precluded by the limitations of the analytical centrifugation method (see [60] for discussion), but it is clear that this simple method gives the potential to "steer" the ZnS QDs for size optimization.

8. Considerations for large scale process using ZnS quantum dots

A comparison was made of the cost/benefit analysis of electricity production based on the microalga *C. vulgaris* (**Table 1**). Open ponds are feasible and are used routinely, with process intensification achieved using raceways (see earlier), but the best photobioreactor format was concluded to be a flat panel arrangement which, although of volume of 20% of that of an open pond, gave >3-fold more biomass production for ~ twice the cost. (**Table 1**), also outperforming a tubular reactor arrangement. Consideration of algal growth for biofuels production has been reviewed elsewhere [69]. Calculations were made here based on using LEDs to boost light delivery, projecting a system of daytime solar irradiation via solar panels (parallel to the PBR) along with modern battery technology (energy storage) to permit LED-illumination (for culture 'tickover') at night (**Table 1**). A full cost-benefit and life cycle analysis is in progress, but here, it should be noted that ZnS quantum dots have also found application in solar cells [70, 71], giving further scope for cost reduction of solar panels which is not factored into **Table 1**. Similarly, **Table 1** does not take into account any increase in photoproductivity via use of QDs, and the values shown (made on the basis of published values) may reveal further benefits (e.g., 2-fold) via addition of the QD technology described here. Hence, the calculations shown in **Table 1** are taken to form a conservative "baseline."

Although immobilized QDs in suspension in a circulating reactor (raceways) might be appropriate for large scale, well-mixed growth, this may give challenges with respect to stability of the encapsulation material under shear, recovery of the QDs, and importantly, ensuring transparency to UV irradiation in the region of interest (absorbance maximum was ~ 310–315 nm with a peak emission at 425 nm; **Figure 4**). This redshift with respect to early work [60] is very relevant: UV light is divisible into UVA (315–400 nm), UVB (280–315 nm), and UVC (100–289 nm). The latter (the most damaging to living cells due to absorbance by DNA and proteins) is almost all absorbed by the atmosphere. Of the total UV radiance reaching the earth's surface, 85% comprises UVA, while only 5% comprises UVB; At 310 nm, the portion

of available sunlight at the earth's surface is ~ half of that obtained at the maximum transmittance of light of ~625 nm [72]. Inspection of **Figure 9** shows that the larger QDs made in 7–10 mM citrate (**Figure 11**) absorb at the interface between UVA and UVB, and further work using lower concentrations of citrate may repay study to redshift both the absorbance and emission peaks by, ideally, a further 5–10 nm. The "preferred" UV light for irradiation also drives the choice of reactor materials (**Table 4**).

From **Table 4**, it is clear that several types of bulk materials would have potential application in large scale photobioreactor technology. LLDPE materials, transparent to both UVA and UVB, are used extensively in bottles and liquid sachets, and a simple approach might involve flotation or suspension of suitable sachet bags into various types of culture as shown in **Figure 2**. However, LLDPE polymers degrade in UV light with a useful life of only about 3 years [73] and would not provide a durable solution, although they would provide a route to easy separation of QDs for re-use. It is also routine to use Perspex™ for photobioreactor materials, e.g., for enclosed inserts. Indeed, Perspex™ is routinely used in numerous applications such as glazing, and its properties are well described, including hardness and scratch resistance; indeed, it is recommended for use as a flooring material [74]. Should scratches occur they can be easily polished out using a proprietary polishing material [74], although the degree of polishing required to achieve a near-perfect optical transmission for optimal use of quantum dots would need to be determined experimentally.

Material	Type	Examples	Transparency UVB	Transparency UVA
Building window materials	Glasses	Clear glass	Opaque	Transparent
		Reflective glass		
		Tinted/wire		
		Tinted glasses		
Nonwindow materials		Quartz glass	Transparent	Transparent
		Perspex	Perspex is the best.	Perspex is the best.
		Furniture glass[1]		
Transparent linear low density polyethylene (LLDPE)	Liquid	Blue crystal	Transparent	Transparent
	Storage bags	"Acqua fil" "Cool Pak"		
	(Sachet bags)	"Ahenpon", "Kenro"		
Polyethylene terephthalate	Plastic bottle	"Standard water"	Opaque	Transparent
	Containers for liquid storage	"Voltic", "Ice Pak"		
		"BelAquah"		
		"Coca Cola"		

Table 4. UV transparency of some common materials used in bulk applications.

9. Conclusions

Photobiotechnologies are maturing rapidly from small-scale high-value applications to large scale operations for biofuels. The major challenge remains optimal use of solar light, since photosynthesis is intrinsically inefficient and effective solar-biotechnologies are currently limited geographically to areas of high and constant solar irradiance. LEDs are already used to supply light into photobioreactors, but their use at large scale requires a careful cost-benefit analysis, especially with regard to the overall energy balance and especially if the biomass is used to make biofuels. Quantum dot technologies, until now used at small scale for niche applications such as imaging, are entering the global commodity market, but traditional QDs are costly. We have shown that commercial QDs can be used to double the photoproductivity, and we also show an economic route to QD manufacture via harnessing a waste from another biotechnology process into the QD manufacturing without compromising quality or performance.

Acknowledgements

We acknowledge the support of NERC (Grant No NE/L014076/1) in the research presented here (AJM and RLO) to develop ZnS-based quantum dots technology via resource recovery from waste. The underpinning evaluation of commercial quantum dots in the three test photobiological systems was supported by the Discipline Hopping Award scheme co-funded by EPSRC, BBSRC, and MRC. The support of BBSRC is acknowledged for MRes studentships (AG and FW). We also thank Drs D.J. Binks and M. Dickinson of the Photonics Institute, University of Manchester, for collaborations, photonics expertise and hosting the secondment of Dr. M.D. Redwood. We acknowledge with thanks the discussions and collaboration with Mr. J. Gomez-Bolivar and Dr. M. Merroun of University of Granada, Spain.

Author details

Angela Janet Murray[1], John Love[2], Mark D. Redwood[1], Rafael L. Orozco[1],
Richard K. Tennant[2], Frankie Woodhall[1], Alex Goodridge[1] and Lynne Elaine Macaskie[1]*

*Address all correspondence to: l.e.macaskie@bham.ac.uk

1 School of Biosciences, University of Birmingham, Edgbaston, Birmingham, UK

2 Biocatalysis Centre, University of Exeter, Exeter, UK

References

[1] Hillen LW. Hydrocracking of the oils of *Botryococcus braunii* to transport fuels. Biotechnology and Bioengineering. 1982;**24**:193-205. DOI: 10.1002/bit.260240116

[2] Alfstad T. World Biofuels Study Scenario Analysis of Global Biofuel Markets. BNL-80238-2000. New York NY, USA: Brookhaven National Laboratory; 2008, 2008

[3] Anon. Ethanol Producer Magazine. Global Renewable Fuels Alliance; 2017. Available from: http://www.ethanolproducer.com/articles/14714/grfa-iea-report-highlights-continued-demand-growth-for-biofuels. www.ethanolproducer.com/articles/14714/grfa-iea-report-highlights-continued-demand-growth-for-biofuels.2017. [Accessed December 19, 2017]

[4] Metzger P, Largeau C. *Botryococcus braunii*: A rich source for hydrocarbons and related ether lipids. Applied Microbiology and Biotechnology. 2005;**66**:486-496. DOI: 10.1007/s00253-004-1779-z

[5] Kunwar B, Deilami SD, Macaskie LE, Wood J, Biller P, Sharma BK. Nanoparticles of Pd supported on bacterial biomass for hydroprocessing crude bio-oil. Fuel. 2017;**209**:449-456. DOI: 10.1016/j.fuel.2017.08.007

[6] Qishen P, Baojiang G, Kolman A. Radioprotective effect of extract from *Spirulina platensis* in mouse bone marrow cells studied by using the micronucleus test. Toxicology Letters. 1989;**48**:165-169. DOI: 10.1016/0378-4274(89)90171-9

[7] Samarth RM, Panwar M, Kumar M, Soni A, Kumar M, Kumar A. Evaluation of antioxidant and radical-scavenging activities of certain radioprotective plant extracts. Food Chemistry. 2008;**106**:868-873. DOI: 10.1016/j.foodchem.2007.05.005

[8] Mumtaz T, Yahaya NA, Abd-Aziz S, Abdul Rahman NA, Yee PL, Shirai Y, Hassan MA. Turning waste to wealth-biodegradable plastics polyhydroxyalkanoates from palm oil mill effluent – A Malaysian perspective. Journal of Cleaner Production. 2010;**18**:1393-1402. DOI: 10.1016/j.jclepro.2010.05.016

[9] Redwood MD, Orozco R, Majewski AJ, Macaskie LE. Electro-extractive fermentation for efficient biohydrogen production. Environmental Science and Technology. 2012;**107**:166-174. DOI: 10.1016/j.biortech.2011.11.026

[10] Redwood MD, Orozco R, Majewski AJ, Macaskie LE. An integrated biohydrogen refinery: Synergy of photofermentation, extractive fermentation and hydrothermal hydrolysis of food wastes. Hydrolysis of Food Wastes. 2012;**119**:384-392. DOI: 10.1016/j.biortech.2012.05.040

[11] Akkerman I, Janssen M, Rocha J, Wijffels RH. Photobiological hydrogen production: Photochemical efficiency and bioreactor design. International Journal of Hydrogen Energy. 2002;**27**:1195-1208. DOI: 10.1016/S0360-3199(02)00071-X

[12] Anon. Sustainable Biofuels: Prospects and Challenges. London UK: Typesetting Clyvedon Press, Cardiff UK: The Royal Society; 2008. ISBN: 9780854036622

[13] van Beilen JB. Why microalgal biofuels won't save the internal combustion machine. Biofuels Bioproducts and Biorefining. 2010;**4**:41-52. DOI: 10.1002/bbb.193

[14] Lizzul AM, Allen MJ. In: Love J, Bryant JA, editors. Biofuels and Bioenergy. pp. 191-211. Wiley on Line Library ISBN: 9781118350560. 2017. pp. 191-211. Ch12. DOI: 10.1002/9781118350553

[15] Lea-Smith DJ, Bombelli P, Dennis JS, Scott SA, Smith AG, Howe CJ. Phycobilisome-deficient strains of *Synechocystis* sp. PCC 6803 have reduced size and require carbon-limiting conditions to exhibit enhanced productivity. Plant Physiology. 2014;**165**:705-714. DOI: 10.1104/pp.114.237206

[16] Suh IS, Lee SB. A light distribution model for an internally radiating photobioreactor. Biotechnology and Bioengineering. 2003;**82**:180-189. DOI: 10.1002/bit.10558

[17] Lee CG. Calculation of light penetration depth in photobioreactors. Biotechnology and Bioprocess Engineering. 1999;**4**:78-81

[18] Richmond A. Biotechnology at the turn of the millennium: A personal view. Journal of Applied Phycology. 2000;**12**:441-451. DOI: 10.1023/A:1008123131307

[19] Carvalho AP, Silva SO, Baptista JM, Malcata FX. Light requirements in microalgal photobioreactors: An overview of biophotonic aspects. Applied Microbiology and Biotechnology. 2011;**89**:1275-1288. DOI: 10.1007/s00253-010-3047-8

[20] Lee YK. Microalgal mass culture systems and methods: Their limitations and potential. Journal of Applied Phycology. 2001;**13**:307-315. DOI: 10.1023/A:1017560006941

[21] Voort MPJ, van der, Vulsteke E, Visser CLM de. Macro-economics of algae products, public output report WP2A7.02 of the EnAlgae project, Swansea. 2015. DOI: http://edepot.wur.nl/347712

[22] Rosenberg JN, Guzman BJ, Oh VH, Mimbela LE, Ghassemi A, Betenbaugh MJ, Oyler GA, Donohue MD. A critical analysis of paddlewheel-driven raceway ponds for biofuel production at commercial scales. Algal Research. 2014;**4**:76-88. DOI: 10.1016/j.algal.2013.11.007

[23] Ugwu CU, Aoyagi H. Microalgal culture systems: An insight into their designs, operation and applications. Biotechnology. 2012;**11**:127-132. DOI: 10.3923/biotech.2012.127.132

[24] Subashchandrabose SR, Ramakrishnan B, Megharaj M, Venkateswarlu K, Naidu R. Consortia of cyanobacteria/microalgae and bacteria: Biotechnological potential. Biotechnology Advances. 2009;**29**:896-907. DOI: 10.1016/j.biotechadv.2011.07.009

[25] de Godos I, Blanco S, García-Encina PA, Becares E, Muñoz R. Long-term operation of high rate algal ponds for the bioremediation of piggery wastewaters at high loading rates. Bioresource Technology. 2009;**100**:4332-4339. DOI: 10.1016/j.biortech.2009.04.016

[26] Bwapwa JK, Jaiyeola AT, Chetty R. Bioremediation of acid mine drainage using algae strains: A review. South African Journal of Chemical Engineering. 2017;**24**:62-70. DOI: 10.1016/j.sajce.2017.06.005

[27] Borowitzka MA. Culturing microalgae in outdoor ponds. In: Anderson RA, editor. Algal Culturing Techniques. Amsterdam: Elsevier Academic Press. 2005. pp 205-218. DOI: 10.1016/B978-012088426-1/50015-9

[28] Chisti Y. Biodiesel from microalgae. Biotechnology Advances. 2007;**25**:294-306. DOI: 10.1016/j.biotechadv.2007.02.001

[29] Eriksen NT. The technology of microalgal culturing. Biotechnology Letters. 2008;**30**: 1525-1536. DOI: 10.1007/s10529-008-9740-3

[30] Glemser M, Heining M, Schmidt J, Becker A, Garbe D, Buchholz R, Brück T. Application of light-emitting diodes (LEDs) in cultivation of phototrophic microalgae: Current state and perspectives. Applied Microbiology and Biotechnology. 2016;**100**(3):1077. DOI: 10.1007/s00253-015-7144-6

[31] Lee CG, Palsson B. High density algal photobioreactors using light emitting diodes. Biotechnology and Bioengineering. 1994;**44**:1161-1167. DOI: 10.1002/bit.260441002

[32] Matthijs HC, Balke H, van Hes UM, Kroon BM, Mur LR, Binot RA. Application of light-emitting diodes in bioreactors: Flashing light effects and energy economy in algal culture (*Chlorella pyrenoidosa*). Biotechnology and Bioengineering 1996;**50**:98-107. DOI: 10.1002/(SICI)1097-0290(19960405)50:1<98::AID-BIT11>3.0.CO;2-3

[33] Sorokin C, Krauss RW. The effects of light intensity on the growth rates of green algae. Plant Physiology. 1958;**33**:109-113. DOI: 10.1104/pp.33.2.109

[34] Vonshak A, Richmond A. Problems in developing the biotechnology of algal biomass production. Plant and Soil. 1985;**89**:123-135. DOI: 10.1007/BF02182239

[35] Redwood MD, Dhillon R, Orozco R, Zhang X, Binks DJ, Dickinson M, Macaskie LE. Enhanced photosynthetic output via dichroic beam-sharing. Biotechnology Letters. 2012; **34**:2229-2234. DOI: 10.1007/s10529-012-1021-5

[36] Redwood MD, Paterson-Beedle M, Macaskie LE. Integrating dark and light bio-hydrogen production strategies: Towards the hydrogen economy. Reviews in Environmental Science and Bio/Technology. 2009;**8**:149-185. DOI: 10.1007/s11157-008-9144-9

[37] Stephen AJ, Archer SA, Orozco RL, Macaskie LE. Advances and bottlenecks in microbial hydrogen production. Microbial Biotechnology. 2017;**10**:1120-1127. DOI: 10.1111/1751-7915.12790

[38] Chen H-B, Wu J-Y, Wang C-F, Fu C-C, Shieh C-J, Chen C-I, Wang C-Y, Liu Y-C. Modeling on chlorophyll a and phycocyanin production by *Spirulina platensis* under various light-emitting diodes. Biochemical Engineering Journal. 2010;**53**:52-56. DOI: 10.1016/j.bej.2010.09.004

[39] Chen SL. The action spectrum for the photochemical evolution of oxygen by isolated chloroplasts. Plant Physiology. 1952;**27**:35-48. DOI: 10.1104/pp.27.1.35

[40] French CS. The rate of CO_2 assimulation by purple bacteria at various wave lengths of light. Journal of General Physiology. 1937;**21**:71-87. DOI: 10.1085/jgp.21.1.71

[41] Haxo FT, Blinks LR. Photosynthetic action spectra of marine algae. Journal of General Physiology. 1950;**33**:389-422. DOI: 10.1085/jgp.33.4.389

[42] Nogi Y, Akiba T, Horikosji K. Wavelength dependence of photoproduction of hydrogen by *Rhodopseudomonas rutila*. Agricultural and Biological Chemistry. 1985;**49**:35-38. DOI: 10.1080/00021369.1985.10866684

[43] Michalet X, Pinaud FF, Bentolila LA, Tsay JM, Doose S, Li JJ, Sundaresan G, Wu AM, Gambhir SS, Weiss S. Quantum dots for live cells, in vivo imaging, and diagnostics. Science. 2005;**307**:538-544. DOI: 10.1126/science.1104274

[44] Anon. Availlable from: https://www.led-professional.com/resources-1/articles/more-efficient-plant-growth-with-quantum-dots-by-nanoco-lighting. [Accessed 22 December 2017]

[45] Coppack DL. The effect of changes in irradiance on the growth, biomass, lipid accumulation and pigment composition of *Botryococcus braunii.* MRes Thesis, University of Exeter, UK. 2013

[46] Frank HA, Polivka T. In: Hynter CN, Daldal F, Thurnauer MC, Beatty JT, editors. Energy Transfer from Carotenoids to Bacteriochlorophylls in the Purple Photosynthetic Bacteria. Dordrecht, The Netherlands: Springer. 2009. pp. 213-230. DOI: 10.1016/0005-2728(90)90194-9

[47] Saer RG, Blakenship RE. Light harvesting in phototrophic bacteria structure and function. Biochemical Journal. 2017;**474**:2107-2131. DOI: 10.1042/BCJ20160753

[48] Qin H, Meng R, Wang N, Peng X. Photoluminescence intermittency and photo-bleaching of single colloidal quantum dot Advanced Materials. 2017;**29**:1606923 DOI: 10.1002/adma.201606923

[49] Garrison TS, Ellis R. Oceanography: An invitation to Marine Science Cengage Learning 20 Channel Center St. Boston MA 02210, USA, 2016

[50] Ňancucheo I, Johnson DB. Selective removal of transition metals from acidic minewaters by novel consortia of acidophilic sulfidogenic bacteria. Microbial Biotechnology. 2012;**5**:34-44. DOI: 10.1111/j.1751-7915.2011.00285.x

[51] Ana Laura Santos AL, Johnson DB. The effects of temperature and pH on the kinetics of an acidophilic sulfidogenic bioreactor and indigenous microbial communities. Hydrometallurgy. 2017;**168**:116-120. DOI: 10.1016/j.hydromet.2016.07.018

[52] Huang J, Yang Y, Xue S, Yang B, Liu S, Photoluminescence SJ. Electroluminescence of ZnS:Cu nanocrystals in polymeric networks. Applied Physics Letters. 1997:2335-2337. DOI: 10.1063/1.118866

[53] Khosravi AA, Kundu M, Jatwa L, Deshpande K, Bhagwart UA, Sastry M, Kulkarni SK. Green luminescence from copper doped zinc sulphide quantum particles. Applied Physics Letters. 1995;**67**:2702-2704. DOI: 10.1063/1.114298

[54] Lai CH, Lu MY, Chen LJ. Metal sulfide nanostructures: Synthesis, properties and applications in energy conversion and storage. Journal of Materials Chemistry. 2012;**22**:19-30. DOI: 10.1039/C1JM13879K

[55] Johnston RJ, Wilcoxon JP. Metal Nanoparticles and Nanoalloys, Vol 3. London: Elvesier; 2012. DOI: 10.1016/B978-0-08-096357-0.00006-6

[56] Dixit N, Soni HP. Tuning optical properties of ZnS nanoparticles in micellar medium at different pH. Superlattices and Microstructures. 2014;**65**:344-352. DOI: 10.1016/j.spmi.2013.11.018

[57] Khani O, Rajabi HR, Yousefi MH, Khosravi AA, Jannesari M, Shamsipur M. Spectrochimica Part A. 2011;**79**:361-369. DOI: 10.1016/j.saa.2011.03.025

[58] Senthilkumar K, Ramamurthi K, Kalaivani T, Balasubramanian V. Indian Journal of Advances in Chemical Science. 2013;**2**:1-5

[59] Mandal A, Dandapat A, De G. Magic sized ZnS quantum dots as a highly sensitive and selective fluorescence sensor probe for Ag^+ ions. The Analyst. 2012;**137**:765-772. DOI: 10.1039/C1AN15653E

[60] Murray AJ, Roussel J, Rolley J, Woodhall F, Mikheenko IP, Johnson DB, Bolivar JG, Merroun ML, Macaskie LE. Biosynthesis of zinc sulfide quantum dots using waste off gas from metal bioremediation process. RSC Advances. 2017;**7**:21484-21481. DOI: 10.1039/C6RA17236A

[61] Anon 2016 Quantum dots are impacting the Emarket. Available from: https://www.printedelectronicsnow.com/issues/2016-0301/view_features/quantum -dots-are-impacting-the-market/46392. [Accessed 26 December 2017]

[62] Benemann JR. Hydrogen production by microalgae. Journal of Applied Phycology. 2000;**2**:291-300. DOI: 10.1023/A:100817511

[63] Melis A. Green alga hydrogen production: Progress, challenges and prospects. International Journal of Hydrogen Energy. 2202;**27**:1217-1228. DOI: 10.1016/S0360-3199(02)00110-6

[64] Modigell M, Holle N. Reactor development for a biosolar hydrogen production process. Renewable Energy. 1998;**14**:421-426. DOI: 10.1016/S0960-1481(98)00098-6

[65] Tredici MR, Zittelli GC, Benemann JR. A tubular integral gas exchange photobioreactor for biological hydrogen production: Preliminary cost analysis. In: Zaborsky OR, Benemann JR, Matsunaga T, Miyake J, San Pietro, editors. Biohydrogen. Amsterdam: Pergamon press, Elsevier; 1999. DOI: 10.1007/978-0-585-35132-2_48

[66] Prahl 2017. Optical Absorption and Emission Data of Chlorophyll a. Available from: http://omlc.org/spectra/PhotochemCAD/html/123.html

[67] Dixon JM, Taniguchi M, Lindsey JS. PhotochemCAD 2. A refined program with accompanying spectral databases for photochemical calculations. Photochemistry and Photobiology. 2005;**81**:212-213. DOI: 10.1111/j.1751-1097.2005.tb01544.x

[68] Prasad PN. Nanophotonics. Hoboken, NJ, USA: John Wiley & Sons; 2004. DOI: 10.1002/047 1670251.ch1

[69] Zittelli GC, Rodolfi L, Bassi N, Tredici M. In: Borowitzka MA, Moheimani N, editors. Photobioreactors for Microalgal Biofuel Production. In: Algae for Biofuels and Energy. New York, USA: Springer; 2013. pp.115-131 Ch7. DOI: 10.1007/978-94-007-5479-9_7

[70] Kim JY, Yang J, Yu JH, Baek W, Lee C, Son HJ, Hyeon T, Ko MJ. Highly efficient copper-indium-selenide quantum dot solar cells: Suppression of carrier recombination by controlled ZnS overlayers. ACS Nano 2015;**9**:11286-11295. DOI: 10.1021/acsnano.5b04917

[71] Labiadh H, Slah Hidouri S. ZnS quantum dots and their derivatives: Overview on identity, synthesis and challenge into surface modifications for restricted applications. Journal of King Saud University – Science. 2017;**29**:444-450. DOI: 10.1016/j.jksus.2016.12.001

[72] Sackey SS, Vowotor MK, Owusu A, Mensah-Amoah P, Tatchie ET, Sefa-Ntiri B, Hood CO, Atiemo SM. Spectroscopic study of UV transparency of some materials. Environment and Pollution. 2015;**4**:1-17. DOI: 10.5539/ep.v4n4p1

[73] Burgess G, Fernández-Velasco JG, Lovegrove K. Materials, geometry, and net energy ratio of tubular photobioreactors for microalgal hydrogen production WHEC 16 / 13-16 June 2006 – Lyon France

[74] Anon. Pespex™ for glazing. PXTD 236 13th Edition. Darwen, Lancs UK: Lucite Internaitonal Ltd.; Available from: http://www.qdplastics.co.uk/assets/docs/Acrylic/Perspex_Glazing_236.pdf